Cognitive Neurodynamics (2019) 13:293–302
https://doi.org/10.1007/s11571-018-9507-z

RESEARCH ARTICLE

Neurodynamic analysis of Merkel cell–neurite complex transduction mechanism during tactile sensing

Mengqiu Yao[2] · Rubin Wang[1,2]

Received: 8 June 2018 / Revised: 27 August 2018 / Accepted: 7 September 2018 / Published online: 22 September 2018

Abstract

The present study aimed to identify the mechanism of tactile sensation by analyzing the regularity of the firing pattern of Merkel cell–neurite complex (MCNC) under the stimulation of different compression depths. The fingertips were exposed to the contact pressure of a spherical object to sense external stimuli in this study. The distribution structure of slowly adapting type I (SAI) mechanoreceptors was considered for analyzing the neural coding of tactile stimuli, especially the firing pattern of SAI neural network for perceiving the external stimulation. The numerical simulation results showed that (1) when the skin was pressed by the same sphere and the depth of the pressing finger skin and position of the force application point remained unchanged, the firing rate of the neuron depended on the synergistic effect of the number of receptors connected with the neuron and the distance between the neuron and the force application point. (2) When the fingertip was pressed by the same sphere at a constant depth and the different contact position, the overall firing rate of the MCNC neural network increased with the number of SAI mechanoreceptors in the area where the force application point was located.

Keywords Merkel cell–neurite complex · SAI mechanoreceptor · Strain energy density · Tactile neural network

Introduction

Hand touching external objects is the major method of tactile sense generation, because there are rich cutaneous mechanoreceptors in hands that can provide physical information of contacted objects to brain. From a biomechanical point of view, when a finger comes into contact with an external object and produces relative motion, the finger skin produces mechanical deformation such as compression and stretching, and the mechanical stimulation receptor located in the deep layer of the skin induces a corresponding action potential. By activating internal ion channel, neurons of the involved mechanoreceptors transfer external physical stimuli into electric signal (Johnson 2001; Maeno et al. 1998). The electric signal is further delivered to nervous system of somatosensory cortex, generating mental health with tactual perception. Human cutaneous mechanoreceptors can be classified as slowly adapting type and rapidly adapting type according to their rates of adaptation. The former corresponds to fast and transient variation of stimulus, and the later corresponds to slow change (Johnson 2001).

A study on tactile receptor neurons (Johansson et al. 1982) found that the firing rates of Merkel cell–neurite complexes (MCNCs) belonged to SAI mechanoreceptors because the mechanoreceptors were sensitive to the features of objects (surface texture and curvature) and had a high spatial resolution. Based on Iggo and Muir's findings, Merkel cell-neurite complexes are thought to be the touch receptors that initiate SAI responses of $\alpha\beta$ afferents for encoding the details of objects (Iggo and Muir 1969) (surface texture and curvature). When the fingertip touched the outline of the object, the SAI mechanoreceptors responded to the skin deformation. Srinivasan and Lamotte (1996) stimulated macaque monkeys (fingertips with a variety of regular geometric objects) and analyzed the

✉ Rubin Wang
rbwang@163.com

[1] College of Computer Science, Hangzhou Dianzi University, Zhejiang, China

[2] Institute for Cognitive Neurodynamics, School of Science, East China University of Science and Technology, Meilong Road 130, Shanghai 200237, China

relationship between the induced firing rate and the deformation components of soft tissue so as to simulate the firing rate of SAI mechanoreceptors to this kind of mechanical stimuli. It was found that the induced firing rate of this tactile receptor was proportional to the maximum tensile strain of the soft tissue in itself and its vicinity. Gerling et al. proposed a combined model of skin mechanics (finite element model, FEM), current transduction and neurodynamics (leaky integrate-and-fire model, LIF) to analyze the evoked firing rate of these tactile receptors (Kim et al. 2010; Gerling and Thomas 2008; Wang et al. 2016). According to Abraira and Ginty (2013), a single neuron could not encode accurate information about the characteristics of external stimuli, but the tactile information could be encoded through a cluster network. Most of the recent studies used the finite element model to transform indentation on the skin's surface into distributions of stress and strain. The corresponding receptor current was calculated using the current transduction model to analyze the firing rate of a single mechanoreceptor neuron under external stimuli. However, the mathematical model could not be used to analyze the other mechanical and physical properties of external stimuli, the spatial distribution of skin tactile receptors, and the dynamic process of neural networks.

The present study focused on the energy transfer and neurodynamics of skin MCNCs under the pressure of spherical objects. Not only the curvature and pressing depth of the force-applying object but also the effect of the number of MCNCs at different locations should be taken into account for encoding an external stimulus to analyze the neural response of fingertip skin to sustained normal compression stimulation. Therefore, based on the findings of Kim et al. (2010), Gerling and Thomas (2008), this paper presented a combined model composed of the model of contact mechanics (Sripati et al. 2006; Hodgkin and Huxley 1990), improved current transduction model, Hodgkin–Huxley model (Phillips and Johnson 1981) of single MCNC, and structural neural network model of MCNC cluster to analyze the neural activity model of SAI mechanoreceptor neuron network. Based on MCNCs cluster, this study investigated mainly two problems: (1) The firing rates of receptor neurons at different locations without changing the indention depth of the skin at the fingertips were related to the shape of the force-applying object and the position of the force application point. (2) The overall distribution of the MCNC network by changing the force application point and not changing the indention depth of the skin at the fingertips and the shape of the force-applying object.

Four kinds of models and methods

Contact mechanics model

The contact mechanics model proposed by Phillips and Johnson is suitable for one-dimensional stimulation (Phillips and Johnson 1981; Shimawaki and Sakai 2007) (for example, grating). In reality, external stimuli should not be limited to one-dimensional. Therefore, the model was extended in this study, where a rigid sphere was pinched at the fingertips as an example. The contact area is generally spatial ellipse, here it is simplified as a concave geometrical shape (Johansson and Vallbo 1980). The deformation and stress distributions of the skin after external stimulation were first calculated to understand the encoding of the external stimuli on the skin.

According to the contact mechanics theory (Sripati et al. 2006), the contact pressure between two objects is shown in Eq. (1). By studying this kind of contact deformation, Johnson obtained the vertical displacement of the surface of the body, namely the closed-form solution of the shape variable (Sripati et al. 2006; Phillips and Johnson 1981), as shown in Eq. (2).

$$p(r,d) = \frac{2E^*}{R^*}\left(a_H^2 - r^2\right)^{1/2} e^{-r^2 F/2.67 a_H} \tag{1}$$

$$U(r) = \begin{cases} \pi p_H \dfrac{2a_H^2 - r^2}{2a_H E^*}, & 0 \le r < a_H \\ \dfrac{p_H}{2a_H E^*}\left[\left(2a_H^2 - r^2\right) sin^{-1}(a_H/r) + \dfrac{r a_H}{2}\sqrt{1-(a_H/r)^2}\right], & r \ge a_H \end{cases} \tag{2}$$

where

$$1/R^* = 1/R_{skin} + 1/R_{mat},\ R^*$$

is the equivalent radius, $a_H = \sqrt{R^* d}$ is the contact radius, $F = 4a^4 E^*/3$ is the force acting on the sphere, $p_H = \frac{2E^*}{\pi a_H}\sqrt{\frac{d}{R^*}}$ is the pressure of the contact center, r is the distance from the force point, $U(r)$ is a skin shape variable at a distance of r mm from the force application point, and

$$E^* = \left(1 - v_{skin}^2\right)/E_{skin} + \left(1 - v_{mat}^2\right)/E_{mat}$$

is the equivalent Young's modulus of two contact objects.

Güçlü et al. (2008) showed that the area of the first knuckle skin was about 4.7 cm^2. On this basis, the first knuckle skin of the index finger was modeled mathematically. For saving calculation cost, in this study the computational area for skin contact was set as 6 cm^2, and the length and width of the calculated area were 30 mm and 20 mm, respectively. Then, the stress and strain of the soft tissue in the area were calculated. MCNCs were located at the epidermal–dermal junction (Maksimovic et al. 2014;

Montagna et al. 1993). The epidermis had the Young's modulus of 1.36 × 10^5 Pa and Poisson's ratio of 0.48, and the dermis had the Young's modulus of 8.00 × 10^4 Pa and Poisson's ratio of 0.48 (Briggaman and Wheeler 1975; Munger and Ide 2011). The equivalent Young's modulus of skin was calculated based on the Young's modulus and Poisson's ratio of the epidermis and dermis.

Current transduction model

When the fingertip touched the outline or edge of an external object and the receptor under the skin was stimulated by pressure, a membrane potential change occurred. The process of converting the change in pressure stimulation into the change in membrane potential was not only a kind of energy transduction but also a process of nerve signal transduction. According to the function of the four kinds of low-threshold mechanoreceptors in tactile discrimination (Johnson 2001; Johnson et al. 2000), slowly adapting type I mechanoreceptor (SAI) was a MCNC located at the epidermal–dermal junction and mainly distributed at the fingertip. It was sensitive to sustained indention (Johansson et al. 1982). Therefore, how the SAI mechanoreceptor converts the external physical stimulus calculated by the contact mechanics model into an electrical signal was the reason for the establishment of the present transduction model.

Previous researchers studied the properties of coded stimuli by recording their neural firing rates by direct mechanical stimulation of the rapidly adapting Pacinian corpuscles (Güçlü and Bolanowski 2002). In contrast, MCNCs were embedded in skin tissue because they were not similar to Pacinian corpuscles. Therefore, no independent MCNC force transduction mechanism existed. Dandekar and Srinivasan expressed the transformation of external physical stimulation by strain energy density in 1997 to better understand the mechanism of force transduction in MCNCs, which had a good prediction for the response of neural activity (Srinivasan and Lamotte 1996). That is, the strain energy density is proportional to the firing rate of the MCNCs. A previous study (Kim et al. 2010) showed that the strain energy density of MCNCs under pressure was closely related to the firing rate of SAI mechanoreceptors. Their skin was stimulated by external stimuli, and the external stimulus properties were studied by means of energy transformation (Kim et al. 2010; Gerling and Thomas 2008; Wang et al. 2016). The formula for calculating the strain energy density follows as:

$$U_0(r) = \frac{3}{4G}\tau_{oct}^2(r) \tag{3}$$

where $U_0(r)$ represents the strain energy density with the skin squeezed within a unit volume of r from the force application point, G represents shear modulus of elasticity, and $\tau_{oct}(r)$ represents the octahedral shear stress at the point, where σ_{xx}, σ_{yy}, and σ_{zz} are normal stresses and where τ_{xy}, τ_{xz}, and τ_{yz} are shear stresses.

$$\tau_{oct}(r) = \frac{1}{3}\sqrt{(\sigma_{xx}-\sigma_{yy})^2+(\sigma_{yy}-\sigma_{zz})^2+(\sigma_{xx}-\sigma_{zz})^2+6(\tau_{xy}^2+\tau_{yz}^2+\tau_{xz}^2)} \tag{4}$$

$$\begin{bmatrix}\sigma_{xx} & \sigma_{xy} & \sigma_{xz}\\ \sigma_{xy} & \sigma_{yy} & \sigma_{yz}\\ \sigma_{xz} & \sigma_{yz} & \sigma_{zz}\end{bmatrix} = \frac{p(r)}{2\pi}\begin{bmatrix}\cos\theta & -\sin\theta & 0\\ \sin\theta & \cos\theta & 0\\ 0 & 0 & 1\end{bmatrix} \begin{bmatrix}\frac{3r^2z}{R^5}-\frac{1-v}{R^2+zR} & 0 & \frac{3rz^2}{R^5}\\ 0 & (1-2v)\left(\frac{1}{r^2}-\frac{z}{r^2R}-\frac{z}{R^3}\right) & 0\\ \frac{3rz^2}{R^5} & 0 & \frac{3r^3}{R^5}\end{bmatrix} \begin{bmatrix}\cos\theta & \sin\theta & 0\\ -\sin\theta & \cos\theta & 0\\ 0 & 0 & 1\end{bmatrix} \tag{5}$$

where $R = \sqrt{r^2+z^2}$, $z = U(r)$, $\theta = 45^\circ$.

The formula for calculating shear Young's modulus G is shown in Eq. (6), where E is the skin's Young's modulus and v is the Poisson's ratio of the skin.

$$G = \frac{E}{1+v} \tag{6}$$

Previous studies Iggo and Muir (1969, Srinivasan and Lamotte (1996) found that the sigmoidal function could be used to transfer strain energy density (SED) generated by the external stimulation of the fingertip skin into the induced current of MCNCs. The formula for converting SED into induced current is shown in Eq. (7) (Gerling and Thomas 2008). Among them, α, λ, and γ are adjustable parameters whose values are adjusted to fit the typical response of SAI mechanoreceptors.

$$I(r) = \alpha\frac{1}{1+e^{\gamma(\lambda-U_0(r))}} \tag{7}$$

The distribution of SAI mechanoreceptors and the minimum threshold of induced displacement were of great importance to the neural coding of external stimuli to describe the transduction current of SAI at different locations of the force point precisely (Gerling 2010). The displacement threshold of SAI afferent nerve stimulation was 1–5 μm (Abraira and Ginty 2013). Therefore, the minimum induced displacement threshold was 5 μm in this study. Güçlü et al. supposed that rapidly adapting (RA) mechanoreceptors followed the uniform, random, and semi-Gaussian distributions from the fingertips to the first knuckles so as to study the coding of skin sensory nerves in

vibration perception (Wheat and Goodwin 2000). The vibration frequency and amplitude of the original stimulus were mostly reproduced using Gaussian distribution. Goodwin et al. observed that SAIs and RAs had similar distribution characteristics (Goodwin and Wheat 1999; Woo et al. 2015). In this study, the Güçlü's method was used to describe the distribution of SAIs in the range of 20×30 mm^2 using the Gaussian function.

In the Cartesian orthogonal coordinate system shown in Fig. 1, the direction of the fingertip was x, and the direction perpendicular to the fingertip was y. The anatomical observation of SAI mechanoreceptors by Goodwin showed that the SAI mechanoreceptors were randomly distributed in the y direction. The distribution density is shown in Eq. (8).

$$f_y(y) = \begin{cases} \frac{1}{20} & 0 \le y \le 20 \text{ mm} \\ 0 & \textit{Other conditions} \end{cases} \tag{8}$$

In the x direction, the SAI mechanoreceptors satisfied the semi-Gaussian distribution, and the distribution function increased to the fingertip, which could be expressed as follows:

$$f_x(x) = \frac{\alpha}{\sigma\sqrt{2\pi}} e^{-x^2/2\sigma^2} + \beta \tag{9}$$

where

$$f_x(0) = \frac{\alpha}{\sigma\sqrt{2\pi}} + \beta = d_{max}$$

$$\lim_{x\to\infty} f_x(x) = d_{min}$$

$$\frac{1}{l}\int_0^l f_x(x)dx = d$$

Here, $d(= 0.75)$ was the number of SAI mechanoreceptors per square millimeter; $d_{max}(= 1.29)$ and $d_{min}(= 0.143)$ were the maximum and minimum numbers of SAI mechanoreceptors per unit square millimeter, respectively; $l(= 30$ mm$)$ and $w(= 20$ mm$)$ were the length and width of the skin area of the fingertips, respectively; and α, β, and σ were three basic parameters; all parameters were solved in the Matlab software. The minimum induced displacement threshold of SAI mechanoreceptor was found to be 5 μm, and the transduction current formula could be rewritten as follows:

$$I(x,y) = \begin{cases} \alpha \dfrac{1}{1 + e^{\gamma(\lambda - U_0(x,y))}} & U(x,y) \ge 5 \text{ μm} \\ 0 & U(x,y) < 5 \text{ μm} \end{cases} \tag{10}$$

where (x, y) were the mechanoreceptor coordinates calculated in accordance with the SAI mechanoreceptor distribution. The coordinates of the applied force point were set to (x_0, y_0), and the distance between the SAI mechanoreceptors and the force application point was expressed as $r = \sqrt{(x - x_0)^2 + (y - y_0)^2}$. $I(x, y)$ was the inductive current of each MCNC.

H–H model of a single MCNC

For single MCNC, leaky integrate and firing model was often used in the previous studies (Wang et al. 2016) to calculate its firing rate which could predict the strength of external stimulation. However, LIF model could not describe the signal transduction mechanism in molecular level. Lumpkin et al. found that the mechanical conduction channels in MCNCs could convert external stimuli into electrical signals, and the electrical currents could activate sodium, potassium, and calcium channels (Kim et al. 2010; Woo et al. 2014, 2015; Marshall and Lumpkin 2012). Then, action potentials were triggered to transmit tactile

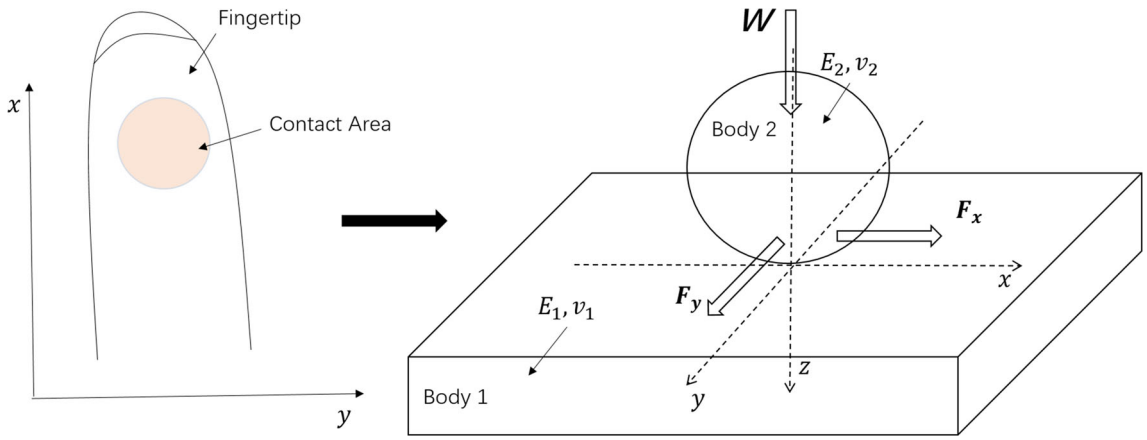

Fig. 1 A simplified model diagram of fingertip contact objects

information to the brain and eventually produce a tactile sensation. Therefore, based on the structure and working principle of MCNCs, an influx of Ca^{2+} ions occurred besides the transport of Na^{+} and K^{+} ions and leakage current (Reid et al. 2003; Tazaki and Suzuki 1998; Chan et al. 1996), as described in the classical H–H model (Phillips and Johnson 1981) when the epidermis was exposed to external stimulation, the stimulated current of this model $I(x, y)$ was calculated using the second model.

Therefore, the differential equations of the H–H model established in this study were modified to the following forms:

$$C_m \frac{dV_m}{dt} = g_l(E_l - V_m) + g_{Na} m^3 h(E_{Na} - V_m) + g_K n^4 (E_K - V_m) + g_{CaL} mh(E_{CaL} - V_m) + I \tag{11}$$

where C_m is the membrane capacitance; V_m is membrane potential; E_{Na}, E_K, and E_{CaL} were the Nernst potentials of sodium, potassium, and calcium, respectively; E_l was the potential with zero leakage current. g_l, g_K, and g_{CaL} were the variable conductance of leakage channel, sodium channel, potassium channel, and calcium channel, respectively (Maio et al. 2016; Wei et al. 2017). The variable conductance of three sample channels was described by a set of nonlinear differential equations:

$$\begin{cases} \frac{dn}{dt} = \alpha_n(1-n) - \beta_n \\ \frac{dm}{dt} = \alpha_m(1-m) - \beta_m \\ \frac{dh}{dt} = \alpha_h(1-h) - \beta_h \end{cases} \tag{12}$$

where

$$\alpha_n = \frac{0.01(10 + V_m - V_r)}{\exp\left[\left(\frac{10+V_m-V_r}{10}\right) - 1\right]};\ \beta_n = 0.125 exp\left(\frac{V_m - V_r}{80}\right)$$
$$\alpha_m = \frac{0.1(25 + V_m - V_r)}{\exp\left[\left(\frac{25+V_m-V_r}{10}\right) - 1\right]};\ \beta_m = 4\exp\left(\frac{V_m - V_r}{18}\right)$$
$$\alpha_h = 0.07\exp\left(\frac{V_m - V_r}{20}\right);\ \beta_h = \frac{1}{\exp\left[\left(\frac{30+V_m-V_r}{10}\right) + 1\right]} \tag{13}$$

where V_r was resting potential.

Network structure model of MCNC cluster

Güçlü et al. observed the distribution of SAI mechanoreceptors in the fingertips of cats and monkeys (Maksimovic et al. 2014) and found that each MCNC was connected with only one SAI fiber, but one SAI nerve fiber was connected with 28 MCNCs on average. The center of the SAI mechanoreceptor or receptive field was distributed parallel to the skin surface. According to Abraira and Ginty (2013), MCNCs did not appear in a single individual form at the epidermal–dermal junction. They were always clustered under the epidermis to receive external stimuli, which were converted into electrical signals. It was transmitted to the cerebral somatosensory cortex via $\alpha\beta$ fibers (Woo et al. 2015; Bessou and Perl 1969; Burgess et al. 1974).Therefore, it was of great significance to construct a network model of MCNC clusters in accordance with the distribution of SAI mechanoreceptors to study the encoding of external stimuli.

The anatomical structure of SAI mechanoreceptors and experimental data showed that the fingertip 20 × 30 mm^2 computing area was divided into 20 subregions of equal area with the length and width of 6 mm and 5 mm, respectively, as shown in Fig. 2. It was assumed that the MCNCs in each subregion were connected to the one end of the same SAI nerve fiber. According to the second model, the number of receptors was not the same for each subregion with the same area.

The other end of the SAI nerve fiber was connected to a neuron, and the neurons in each subregion were labeled with 1–20. Each neuron was connected only with the neurons in the adjacent subregion. Orange lines are used in Fig. 2 to indicate the existence of the connection. The connection between the two neurons meant that the two neurons were coupled and bidirectional, and the coupling intensity between the two neurons was assumed to be equal. In a statistical sense, the range of synaptic coupling strength between neurons was from the random value of uniform distribution (Rubinov et al. 2011; Aouiti 2016; Peters et al. 2017; Manivannan et al. 2016; Mizraji and Lin 2017). Based on the data provided in a large number of published studies, it was assumed that the values were randomly distributed in the range of 0.1–0.3. The final

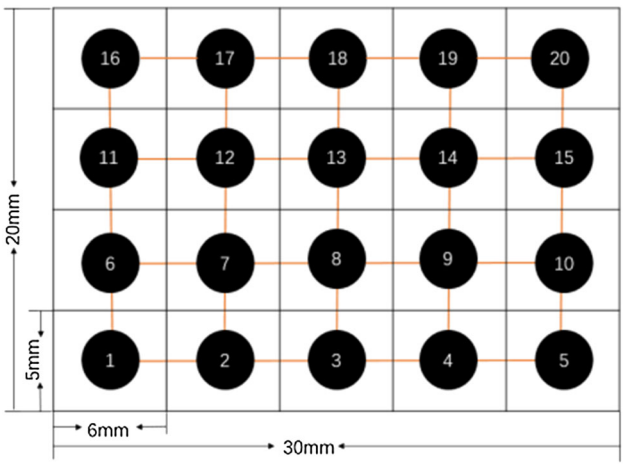

Fig. 2 Schematic diagram of a structural network of the Merkel cell–neurite complex of glabrous skin

value of the connection weight between neurons is determined by the overall firing rate of the network. In this study, a network structure consisting of 20 neurons was constructed. The stimulation current of the *i*th neuron was equal to the sum of the transduction currents generated by all MCNCs in the subregion, as shown in Eq. (14). The average distance between the MCNCs connected by the *i*th neuron and the force application point was calculated, which was used as the distance between the *i*th neuron in the region and the force application point, as shown in Eq. (15).

$$I_i = \sum_{k=1}^{N_i} I\left(x_{i,k}, y_{i,k}\right)(i = 1, 2, \ldots, 20) \tag{14}$$

$$R_i = \frac{\sum_{k=1}^{N_i} \sqrt{\left(x_{i,k} - x_0\right)^2 + \left(y_{i,k} - y_0\right)^2}}{N_i} \ (i = 1, 2, \ldots, 20) \tag{15}$$

where $N_i(i = 1, 2, \ldots, 20)$ was the number of MCNCs connected by the *i*th neuron.

Simulation and result analysis

Based on the neural dynamic combination of contact mechanics, current conversion, and skin mechanoreceptor-induced response, the coding method for the overall firing rate of MCNC cluster network and the position of application points of objects was further studied. As a preliminary exploration, the evoked neural response model of the neural network under the same stimulus intensity and different force application points was calculated.

Modeling verification

First, the same one-dimensional stimulation (grating) as in Phillips and Johnson experiments was used to squeeze the skin, as shown in Fig. 3b, to verify the combined model proposed in this study. The depth of squeezing skin was 1000 μm. The grating width used in model validation was 5 mm, the first adjacent grating spacing was 3 mm, and the second adjacent grating spacing was 5 mm, as shown in Fig. 3b. By combining the first three models to calculate the firing rate of SAI mechanoreceptors at different locations, the simulation results shown in Fig. 4 indicated that the firing rate of the mechanoreceptor neuron in the edge area pressed into the grating was obviously higher than that in the nonedge area. This was because SAI mechanoreceptors were sensitive to external stimuli, consistent with the experimental results in Fig. 3a (Phillips and Johnson 1981).

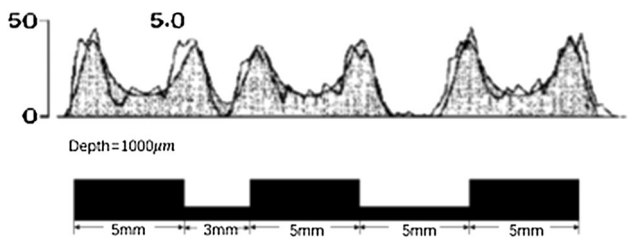

Fig. 3 Firing rates of SAI mechanoreceptors at different locations

Diagram stimulation of strain energy density and distance

As shown in Fig. 5, sphere with 5 mm radius is used to squeeze skin, and the pressed depth is changed to perform numerical simulation and obtain corresponding correlation diagram between strain energy density(SED) and the force application point. For the same calculation area, the external stimuli in Fig. 5 are 1, 2, 3, 4, and 5 mm. It could be observed that (1) the minimum value of SED increases with external stimuli (pressed depth). When the vertical deformation of skin is 0, the corresponding SED is 0. The appearance of the second peak in SED attributes to the elasticity of skin. When the skin is squeezed, the skin will sink. However, the skin not contact with external stimuli will show bump. Therefore, in the range beyond contact radius, the SED is still higher than 0 within a small range. (2) The pressed volume of sphere increases with pressed depth. It means that the external stimuli width becomes wide, and the curve of SED also changes. Relative to radius of applied sphere, when the pressed depth is smaller, the highest point of SED is in the largest deformation quantity. When the pressed depth gradually increases, the SED in the largest deformation quantity gradually decreases. The curve of SED changes from sharp peak into sunk shape, which is in line with Johanson's result (Phillips and Johnson 1981).

The firing pattern of SAI mechanoreceptor neurons under the same sustained pressure and same force point

The force application point used in this simulation study was located at the center of the calculation area of 20×30 mm^2 to simplify the model. Also, the skin was squeezed with a sphere of 2 mm radius, and the extrusion depth was 1.5 mm. The firing rate of neurons in different subregions, the average distance from the force application point, and the number of Merkel cells connected by each neuron were calculated. The relationship between the response of SAI receptors neurons in different subregions and the average distance of the force application point was analyzed to explore the effect of these two factors on the

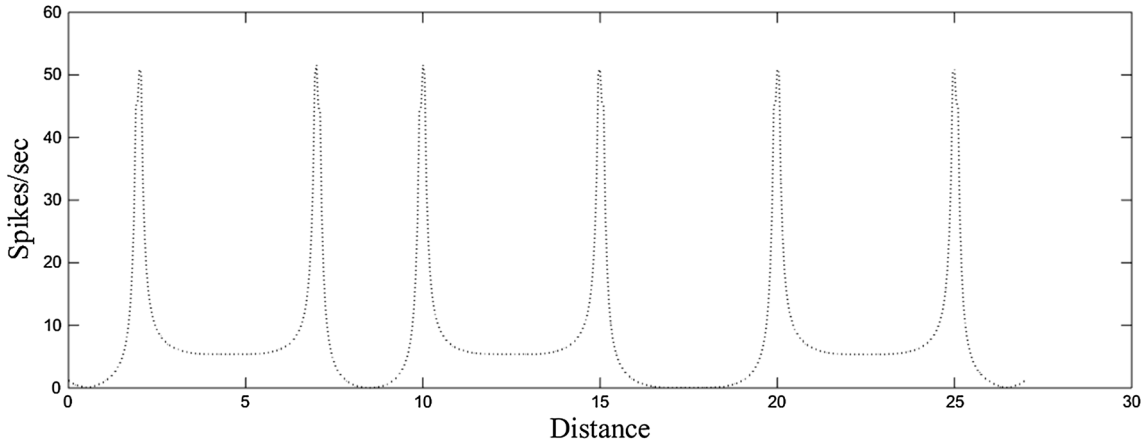

Fig. 4 Firing rates of MCNCs at different locations

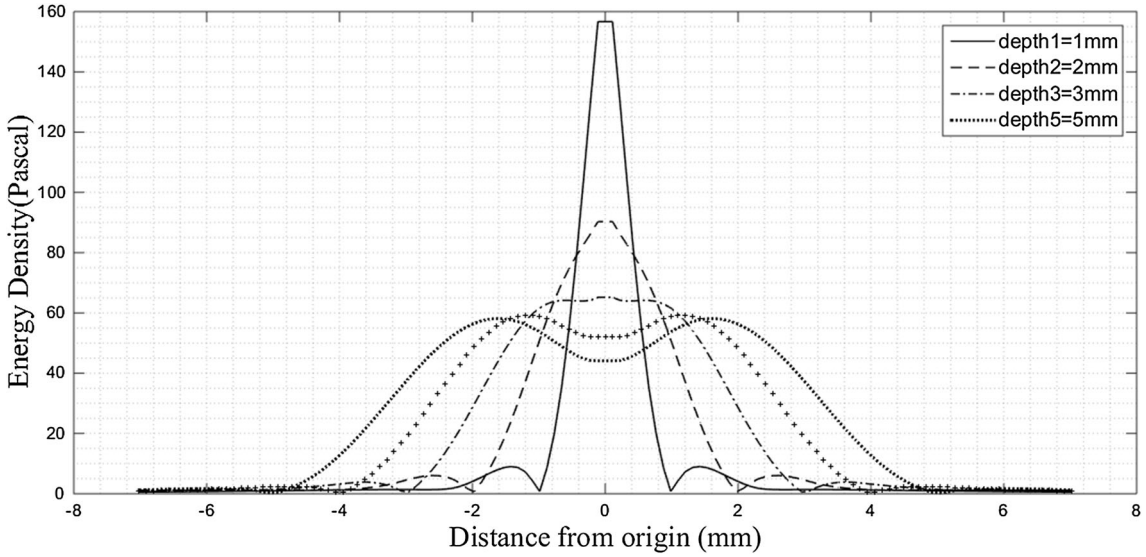

Fig. 5 Strain energy density distribution under different pressed depths in skin

encoding of SAI mechanoreceptor neurons, as shown in Fig. 6. Further, the relationship between the response of SAI mechanoreceptor neurons and the number of Merkel cells connected by each neuron was analyzed in different subregions, as shown in Fig. 7. All raw data were standardized within the range of [0, 1] to analyze the firing rate of SAI mechanoreceptor neurons, the distance between the neurons and the force application points, and the number of Merkel cells connected by SAI mechanoreceptor neurons in the same range. The division of the subregions in Fig. 2 indicated that the force application point was closer to the number 8 and 13 neurons than the neurons in the other subregions. Figure 6 shows that the firing rate of the number 13 neuron was the highest, but the firing rate of the number 8 neuron was not the second highest. Although the average distance from the points of number 18 neuron to the force application point was greater than the average distance from the points of number 8 neuron, the firing rate of the former was greater than that of the latter, indicating that the distance from the point of action to the force application point was not the only factor affecting the firing rate. Figure 7 shows that the number of Merkel cells connected by number 18 neuron was greater than the number of Merkel cells connected by number 8 neuron. Consequently, the firing rate of number 18 neuron far away from the force application point was slightly higher than that of number 8 neuron. These findings suggested that the firing rate of neurons depended on the combination of the number of mechanoreceptors and the distance from the stimuli, explaining the difference in the discriminative ability of different regions of the finger under the same stimulus.

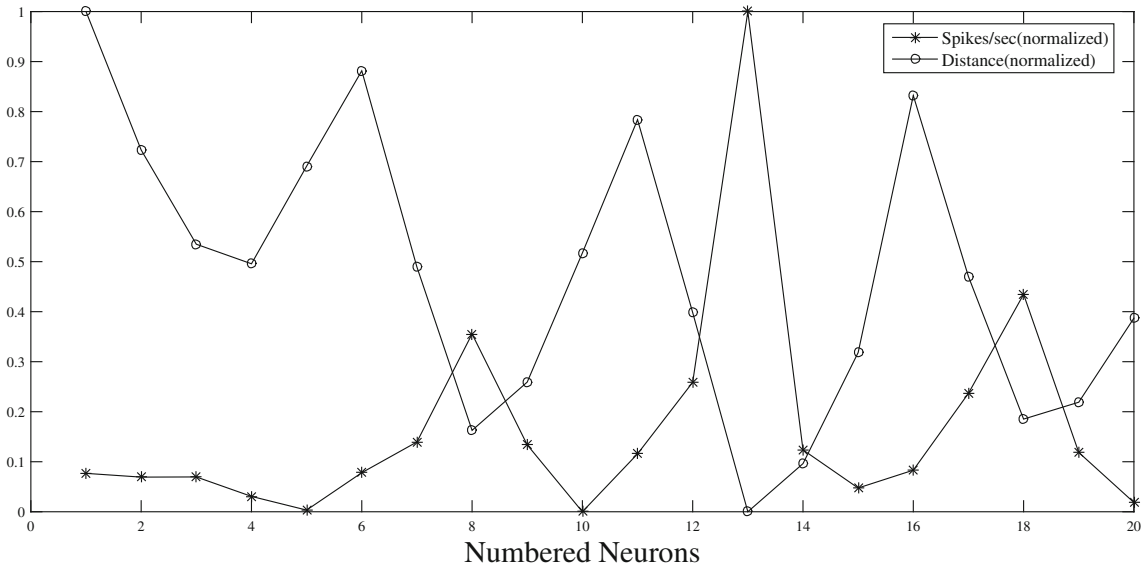

Fig. 6 Relationship between the firing rate and different neurons under the same stimulus

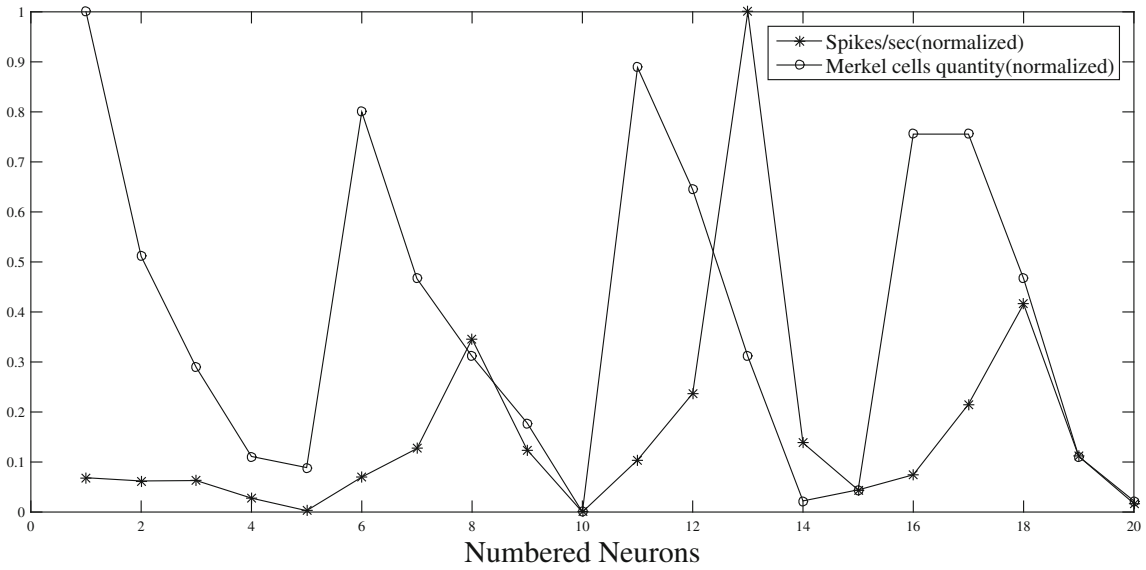

Fig. 7 Relationship between firing rates of different neurons and the number of connected receptors under the same stimulus

Firing pattern of SAI mechanoreceptor neural network under the same sustained pressure and different force points

The experience of external stimulation on touching objects in different positions of fingertips was different. To explore this difference, the geometric center points of 20 different subregions in Fig. 2 were selected as 20 different positions of force points for the simulation experiment. The number was consistent with the number of neurons in the subregion. A sphere with a radius of 2 mm was still used to squeeze the skin with a depth of 1.5 mm. The relationship between the response of the MCNC neural network and the number of receptors in the subregion of the force point was analyzed according to different force application points. Figure 8 shows that the number of Merkel cells in the subregion of the force application point directly affected the response of the neural network. The firing rate of the whole neural network increased with the number of Merkel cells in the subregion of the force application point. On the contrary, the firing rates of the whole neural network decreased with the number of Merkel cells in the subregion of the force application point.

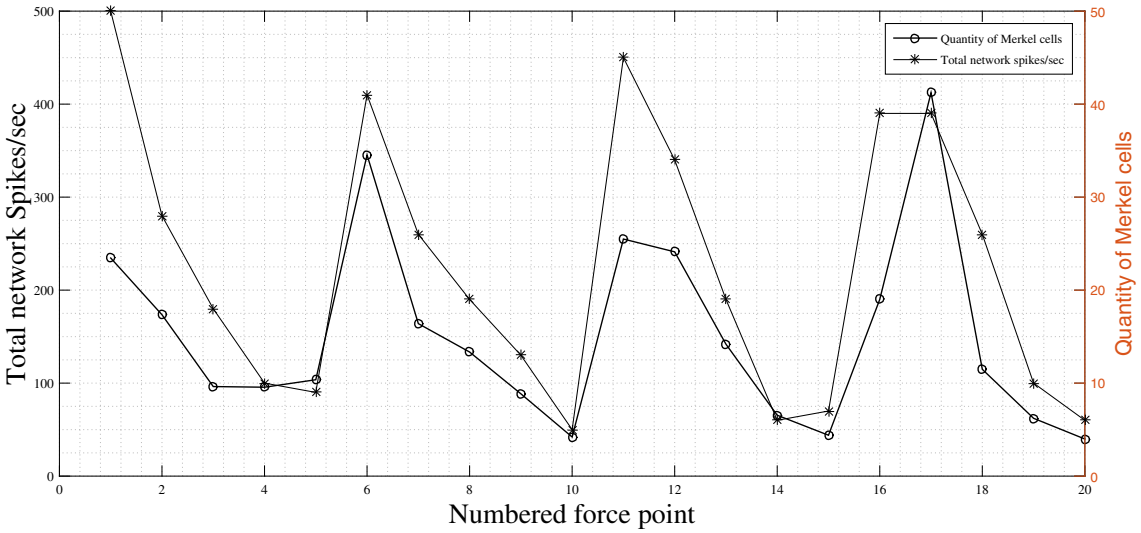

Fig. 8 Relationship between firing rates of MCNC neural network and the quantity of Merkel cells in the subregion of different force application point

Conclusions

The relationship between the deformation of the anterior fingertip under the spherical normal force and the firing rates was quantitatively analyzed and calculated by numerical simulation in this study based on the neural network model of the Merkel cell–neurite complexes at the fingertip. The conclusions were as follows:

1. Due to the elastic properties of fingertip skin, the strain energy density curve obtained by numerical calculation accorded with the curve model of skin deformation obtained by measurement. The comparison revealed that the amplitude of strain energy density increased when the force sphere with a smaller radius and the force sphere with a larger radius acted on the same indentation depth under different stimuli.
2. When the skin was pressed by the same sphere, and the depth of the pressing finger skin and the position of the force application point remained unchanged, the firing rate of the neuron depended on the number of receptors connected by the neuron and the synergistic effect of the distance between the neuron and the force application point. The model proposed in this paper considers the distribution of fingertips of MCNC, so the discharge rate of neurons is not only affected by the physical properties of external stimuli, but also by the distribution of subcutaneous receptors. The combination of these two effects can have a nonlinear effect on the discharge rate of neurons.
3. When the skin was pressed by the same sphere, the depth of the pressing finger skin was constant, and the position of the force application point changed, the overall firing rate of the SAI mechanoreceptor neurons increased with the number of the SAI mechanoreceptors in the area where the force application point was located.

Acknowledgements This work was supported by the National Natural Science Foundation of China (NSFC) (11232005, 11472104, 61633010, 61473110).

References

Abraira VE, Ginty DD (2013) The sensory neurons of touch. Neuron 79(4):618–639

Aouiti C (2016) Neutral impulsive shunting inhibitory cellular neural networks with time-varying coefficients and leakage delays. Cogn Neurodyn 10(6):573–591

Bessou P, Perl ER (1969) Response of cutaneous sensory units with unmyelinated fibers to noxious stimuli. J Neurophysiol 32(6):1025–1043

Briggaman RA, Wheeler CE Jr (1975) The epidermal-dermal junction. J Investig Dermatol 65(1):71–84

Burgess PR, Howe JF, Lessler MJ et al (1974) Cutaneous Receptors supplied by myelinated fibers in the cat. II. number of mechanoreceptors excited by a local stimulus. J Neurophysiol 37(6):1373–1386

Chan E, Yung WH, Baumann KI (1996) Cytoplasmic Ca^{2+} concentrations in intact merkel cells of an isolated, functioning rat sinus hair preparation. Exp Brain Res 108(3):357–366

Gerling GJ (2010) SA-I mechanoreceptor position in fingertip skin may impact sensitivity to edge stimuli. Appl Bion Biomech 7(1):19–29

Gerling GJ, Thomas GW (2008) Fingerprint lines may not directly affect SAI mechanoreceptor response. Somatosens Mot Res 25(1):61–76

Goodwin A, Wheat H (1999) Effects of nonuniform fiber sensitivity, innervation geometry, and noise on information relayed by a population of slowly adapting type I primary afferents from the fingerpad. J Neurosci 19(18):8057–8070

Güçlü B, Bolanowski SJ (2002) Modeling population responses of rapidly-adapting mechanoreceptive fibers. J Comput Neurosci 12(3):201–218

Güçlü B, Mahoney GK, Pawson LJ et al (2008) Localization of merkel cells in the monkey skin: an anatomical model. Somatosens Res 25(2):123–138

Hodgkin AL, Huxley AF (1990) A quantitative description of membrane current and its application to conduction and excitation in nerve. Bull Math Biol 52(1):25–71

Iggo A, Muir AR (1969) The structure and function of a slowly adapting touch corpuscle in hairy skin. J Physiol 200(3):763–796

Johansson RS, Vallbo AB (1980) Spatial properties of the population of mechanoreceptive units in the glabrous skin of the human hand. Brain Res 184(2):66–353

Johansson RS, Landström U, Lundström R (1982) Sensitivity to edges of mechanoreceptive afferent units innervating the glabrous skin of the human head. Brain Res 244(1):27–35

Johnson KO (2001) The roles and functions of cutaneous mechanoreceptors. Curr Opin Neurobiol 11(4):455–461

Johnson KO, Yoshioka T, Vegabermudez F (2000) Tactile functions of mechanoreceptive afferents innervating the hand. J Clin Neurophysiol 17(6):539–558

Kim EK,Gerling GJ,Wellnitz SA et al (2010) Using force sensors and neural models to encode tactile stimuli as spike-based responses. In: Proceedings of Symposium Haptic Interface Virtual Environment and Teleoperator Systems, 2010, pp 195–198

Maeno T, Kobayashi K, Yamazaki N (1998) Relationship between the structure of human finger tissue and the location of tactile receptors. JSME Int J Ser C Mech Syst Mach Elem Manuf 41(2):566–573

Maio VD, Ventriglia F, Santillo S (2016) A model of cooperative effect of AMPA and NMDA receptors in glutamatergic synapses. Cogn Neurodyn 10(4):315–325

Maksimovic S, Nakatani M, Baba Y et al (2014) Epidermal merkel cells are mechanosensory cells that tune mammalian touch receptors. Nature 509(7502):617–621

Manivannan R, Samidurai R, Cao J et al (2016) New delay-interval-dependent stability criteria for switched Hopfield neural networks of neutral type with successive time-varying delay components. Cogn Neurodyn 10(6):543–562

Marshall KL, Lumpkin EA (2012) The molecular basis of mechanosensory transduction. Adv Exp Med Biol 739:142–155

Mizraji E, Lin J (2017) The feeling of understanding: an exploration with neural models. Cogn Neurodyn 11(2):135–146

Montagna W, Kligman AM, Ms KSC (1993) Atlas of normal human skin. Springer, Berlin

Munger BL, Ide C (2011) The structure and function of cutaneous sensory receptors. Arch Histol Cytol 51(1):1–34

Peters JF, Tozzi A, Ramanna S et al (2017) The human brain from above: an increase in complexity from environmental stimuli to abstractions. Cogn Neurodyn 11(4):391–394

Phillips JR, Johnson KO (1981a) Tactile spatial resolution. III. A continuum mechanics model of skin predicting mechanoreceptor responses to bars, edges, and gratings. J Neurophysiol 46(6):1204–1225

Phillips JR, Johnson KO (1981b) Tactile spatial resolution. II. neural representation of bars, edges, and gratings in monkey primary afferents. J Neurophysiol 46(6):1192–1203

Reid CA, Bekkers JM, Clements JD (2003) Presynaptic Ca^{2+} channels: a functional patchwork. Trends Neurosci 26(12):683–687

Rubinov M, Sporns O, Thivierge JP et al (2011) Neurobiologically realistic determinants of self-organized criticality in networks of spiking neurons. PLoS Comput Biol 7(6):e1002038

Shimawaki S, Sakai N (2007) Quasi-static deformation analysis of a human finger using a three-dimensional finite element model constructed from Ct images. J Environ Eng 2(1):56–63

Srinivasan MA, Lamotte RH (1996) Abilities and mechanisms. Tactual Discrimination of Softness. Birkhäuser, Basel, pp 123–135

Sripati AP, Bensmaia SJ, Johnson KO (2006) A continuum mechanical model of mechanoreceptive afferent responses to indented spatial patterns. J Neurophysiol 95(6):3852–3864

Tazaki M, Suzuki T (1998) Calcium inflow of hamster merkel cells in response to hyposmotic stimulation indicate a stretch activated ion channel. Neurosci Lett 243(1):69–72

Wang Y, Baba Y, Lumpkin EA et al (2016) Computational modeling indicates that surface pressure can be reliably conveyed to tactile receptors even amidst changes in skin mechanics. J Neurophysiol 116(1):218–228

Wei H, Bu Y, Dai D (2017) A decision-making model based on a spiking neural circuit and synaptic plasticity. Cogn Neurodyn 11(5):415–431

Wheat HE, Goodwin AW (2000) Tactile discrimination of gaps by slowly adapting afferents: effects of population parameters and anisotropy in the fingerpad. J Neurophysiol 84(3):1430–1444

Woo SH, Ranade S, Weyer AD et al (2014) Piezo2 is required for merkel-cell mechanotransduction. Nature 509(7502):622–626

Woo SH, Lumpkin EA, Patapoutian A (2015) Merkel cells and neurons keep in touch. Trends Cell Biol 25(2):74–81